BEAM DYNAMICS DESIGN OF THE ANNULAR-COUPLED-STRUCTURE LINAC AND ITS BEAM MATCHING SECTION FOR THE KEK/JAERI JOINT PROJECT

Masanori Ikegami, Takao Kato, KEK, Tsukuba, Ibaraki 305-0801, Japan
K. Hasegawa, JAERI, Tokai, Naka, Ibaraki 319-1195, Japan

Abstract

The construction of the high-intensity proton accelerator facility in Japan has been started. We adopt ACS (Annular-Coupled-Structure linac) for the high energy part of the injector linac. The fundamental beam dynamics design of the ACS and its preceding beam matching section is completed. In this paper, we show the outline of the beam dynamics design together with the simulation results with 3D PARMILA.

1 INTRODUCTION

The construction of the high-intensity proton accelerator facility in Japan has been started as a joint project of KEK and JAERI [1]. The facility consists of a 400-MeV injector linac, a 3-GeV RCS (Rapid Cycling Synchrotron), and a 50-GeV main ring. The injector linac for the facility is comprised of a 3-MeV RFQ, a 50-MeV DTL, a 190-MeV SDTL (Separated-type DTL) [2], and a 400 MeV ACS (Annular-Coupled-Structure linac) [3, 4]. The layout of the injector linac is schematically shown in Fig. 1. In this paper, the beam dynamics design of the ACS and the beam matching section between the SDTL and the ACS are presented. While the operation frequency of the low-energy part, which includes the RFQ, the DTL, and the SDTL, is set to 324 MHz, we adopt three-fold frequency jump for ACS to improve the acceleration efficiency. The primary role of the matching section, which is referred to as MEBT2, is to achieve precise and smooth beam matching between the SDTL and the ACS, absorbing the effects of the frequency jump.

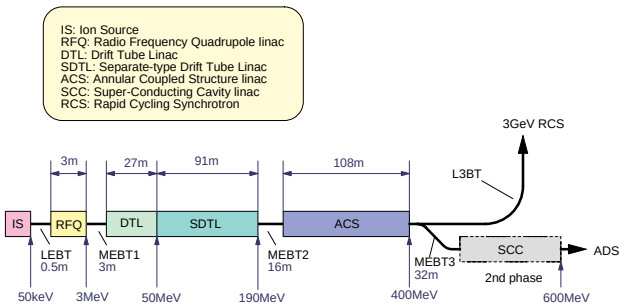

Figure 1: Layout of the injector linac.

Table 1: Main specifications of the ACS

Input beam energy	190.8 MeV
Output beam energy	400 MeV
Operation frequency	972 MHz
Beam particle	Negative hydrogen ion
Peak beam current	50 mA
Pulse width	0.5 msec
Repetition	50 Hz
Num. of cells per tank	15
Num. of tanks per module	2
Num. of modules	23
Num. of klystrons	23
Inter-tank spacing	$4.5\beta\lambda$
Bore radius	20 mm
Average accelerating field E_0	4.26 MV/m
Synchronous phase	-30 deg
Max. surface field	0.85 Kilpatrick
Peak rf power	43.8 MW
Peak wall loss	33.4 MW
Peak beam loading	10.4 MW
Total length	108.3 m

2 ACS LINAC

ACS is a variety of coupled-cavity linacs, which is operated with the $\pi/2$ mode. The distinctive feature of ACS is its coupling cell geometry, which is annular and has the axial symmetry with respect to the beam axis. Because of this geometry, coupling slots, which connects a coupling cell and an accelerating cell, can be located symmetrically. In our design, we have four coupling slots between an accelerator cell and a coupling cell with the four-fold rotational symmetry. This symmetry is expected to suppress the dipole component of the accelerating field in the vicinity of the beam axis [4].

The ACS linac has been developed based on the 1296 MHz ACS model [4], which was developed for the JHP project. The geometry has been optimized to minimize the increase of cavity dimensions due to alteration of the operation frequency. For the details of the cavity design and development, refer to the reference [5].

Our ACS linac consists of 23 ACS modules and accelerates negative hydrogen ions from 190 MeV to 400 MeV. An ACS module consists of two ACS tanks and a bridge coupler connecting them as is shown in Fig. 2. An ACS module is driven by a 2.5-MW klystron, and the rf power is

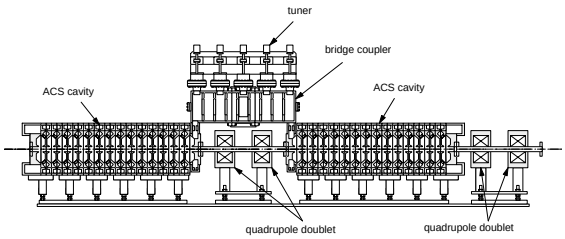

Figure 2: Layout of an ACS module.

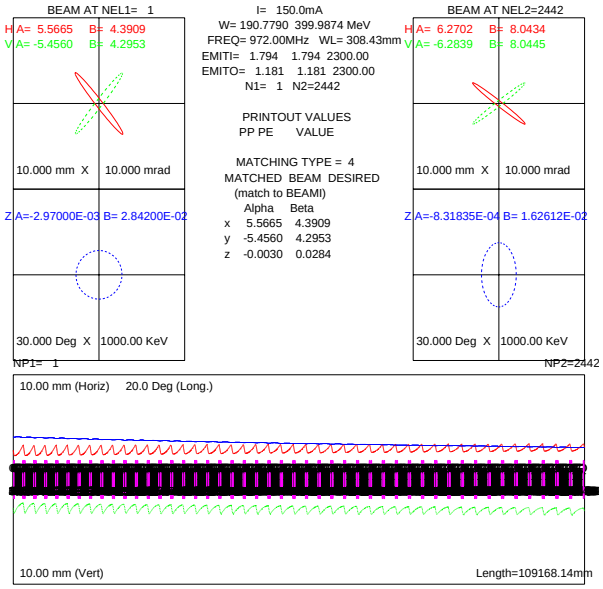

Figure 3: Trace3D result for the ACS.

fed through rf window which is located in the middle of the bridge coupler. An ACS tank contains 15 accelerating cells, 14 coupling cells, and two end-coupling cells. The bridge coupler has disk-loaded structure, and has nine cells. The bridge coupler is also operated with the $\pi/2$ mode.

The inter-tank spacing is $4.5\beta\lambda$, with β and λ being the particle velocity scaled by the speed of light and the rf wave length, respectively. A quadrupole doublet is placed in the inter-tank spacing for transverse focusing. The equipartition condition can be satisfied with the quadrupole doublets for wide range of input emittance.

Table 1 shows the main specifications of the ACS linac. These parameters have been determined considering available rf power and geographical limitations. The beam envelope along the ACS calculated with Trace3D [7] is shown in Fig. 3, in which quadrupole strength is set to satisfy the equipartition condition.

3 MEBT2

MEBT2 is a 15.9 m long beam transport line which is located between the SDTL and the ACS. The main purpose of MEBT2 is to achieve precise beam matching between the SDTL and the ACS. The longitudinal matching

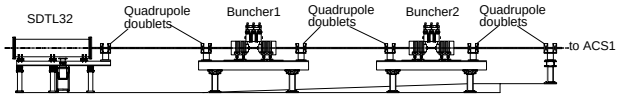

Figure 4: Layout of MEBT2.

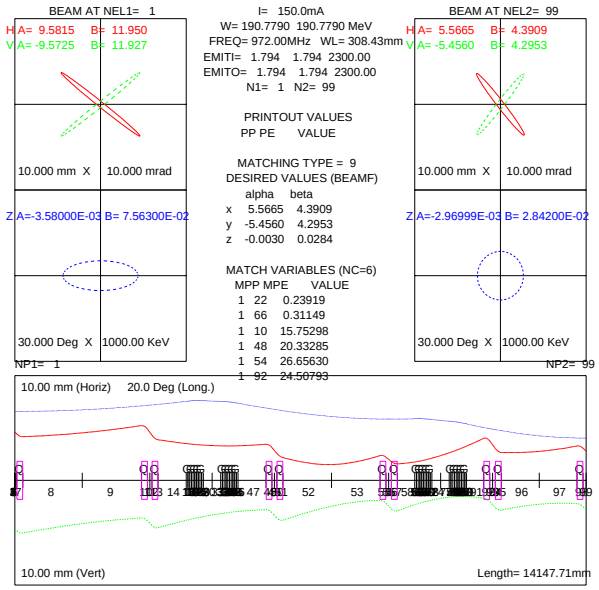

Figure 5: Trace3D result for MEBT2.

is performed with two 972-MHz buncher modules. The buncher modules are ACS type, and they are basically the same with the ACS accelerator modules except the number of cells contained in one tank and the inter-tank spacing. One buncher module consists of two ACS tanks connected with a bridge coupler. One ACS tank contains five accelerating cells, and a bridge coupler has five bridge cells. The inter-tank spacing is $2.5\beta\lambda$.

The transverse matching is performed with 12 quadrupole magnets. While doublet focusing lattice is adopted both in the SDTL and the ACS, the focusing period length is different. Then, "quasi-doublet focusing lattice" is adopted for MEBT2, in which the focusing period is gradually decreased along the beam line. Figure 4 shows the layout of MEBT2, and Fig. 5 shows the beam envelope along MEBT2 calculated with Trace3D. In Fig. 5, the beam evolution is calculated from the center of the first doublet to the center of the last one. As demonstrated in Fig. 5, smooth matching is achieved for a wide range of emittance and beam current, adopting this lattice.

4 PARTICLE SIMULATION

The beam evolution along MEBT2 and the ACS has been simulated with PARMILA [8]. In the simulation, 3D particle-in-cell routine, PICNIC, has been used. The number of meshes are set to $40 \times 40 \times 40$, and 100,000 particles are employed. The 6D waterbag distribution is assumed at

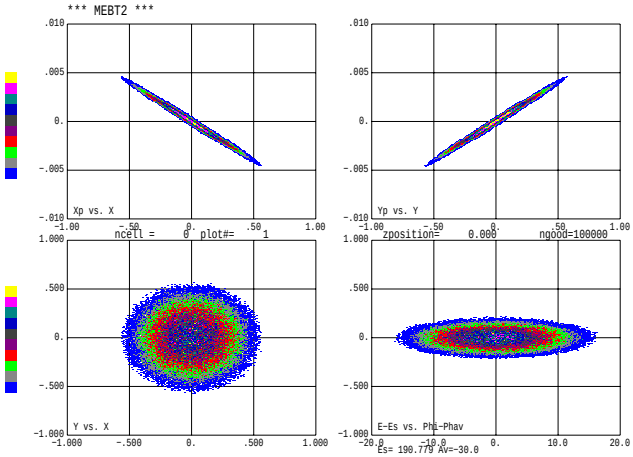

Figure 6: Phase-space distribution at the entrance of the MEBT2. In the top two figures, the horizontal axis is in cm, and the vertical one in rad. In the bottom right figure, the horizontal axis is in degree, and the vertical one in MeV.

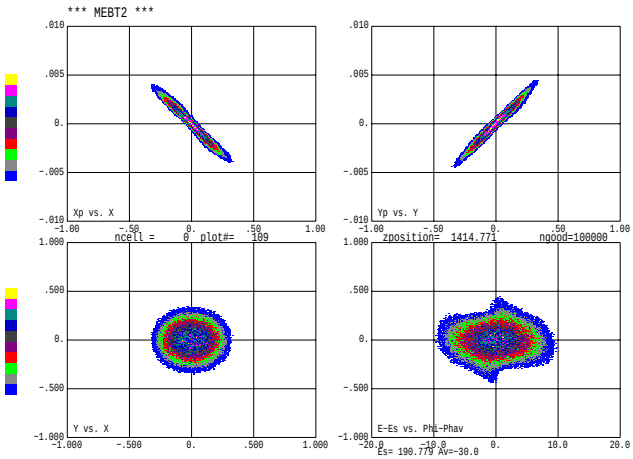

Figure 7: Phase-space distribution at the entrance of the ACS.

the entrance of MEBT2, and no error is applied.

Figures 6 to 8, respectively, show the phase-space beam distribution at the entrance of MEBT2, the entrance of the ACS, and the exit of the ACS. As shown in Figs. 7 and 8, some filamentation has been occurred possibly due to the nonlinearity of the rf field at MEBT2 bunchers. The obtained longitudinal emittance growth rate along MEBT2 and the ACS is 4 % in rms and 24 % in 99 % emittance. As 99 % emittance oscillates along the ACS due to filamentation, we here define that the 99 % emittance growth ratio is the ratio between the maximum 99 % emittance recorded in the ACS and the initial one. Considering that the above defined 99 % emittance growth ratio tends to overestimate the effect of filamentation, we conclude that the obtained result is sufficient. As for the transverse direction, the emittance growth ratio is 6 % in rms, and 24 % in 99 % emittance.

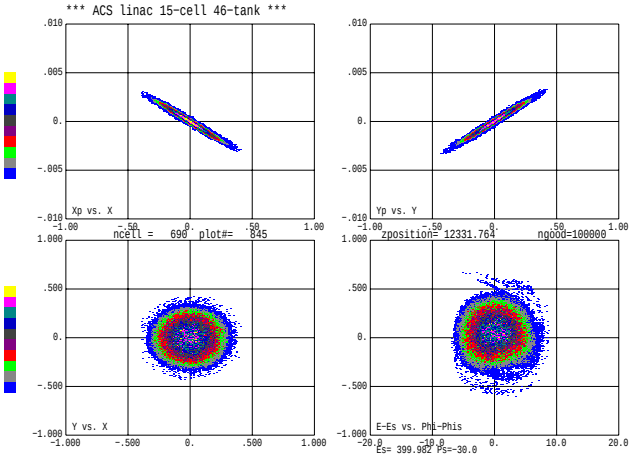

Figure 8: Phase-space distribution at the exit of the ACS.

5 SUMMARY

Beam dynamics design of the ACS linac and the preceding beam matching section has been performed. The beam evolution along the ACS and the matching section has been simulated with PARMILA utilizing a 3D particle-in-cell routine. While some filamentation is observed in the simulation, the obtained results is sufficient. We are planning to proceed to a systematic error study.

6 REFERENCES

[1] F. Naito et. al., in these proceedings.

[2] T. Kato, "Proposal of a Separate-type Proton Drift Tube Linac for Medium Energy Structure", KEK Report 92-10 (1992).

[3] V. G. Andrerev et. al., "Study of High Energy Proton Linac Structures", Pros. of the 1972 Proton Linear Accelerator Conference, 114 (1972); R. A. Hoffswel and R. M. Laszewski, "Higher Modes in the Coupling Cells of Coaxial and Annular-Ring Coupled Linac Structures", IEEE Trans. Nucl. Sci. NS-30, 3588 (1983).

[4] T. Kageyama et. al., "Development of Annular Coupled Structure", Procs. of the 1994 Linear Accelerator Conference, 248 (1994).

[5] V. V. Paramonov, "The Annular Coupled Structure Optimization for JAERI/KEK Joint Project for High Intensity Proton Accelerators", KEK Report 2001-14 (2001); N. Hayashizaki et. al., in these proceedings; H. Ao et. al., in these proceedings.

[6] R. A. Jameson, " Beam Intensity Limitations in Linear Accelerators", IEEE Trans. Nucl. Sci. NS-28, 2408 (1981); M. Reiser, "Theory and Design of Charged Particle Beams", John Willy and Sons, 1994.

[7] K. R. Crandall, "TRACE: An Interactive Beam Dynamics Code", in *Linear Accelerator and Beam Optics Codes*, ed. C. R. Eminheiser, AIP Conference Procs. 177, 29 (1988).

[8] H. Takeda, "PARMILA", Los Alamos National Laboratory Report, LA-UR-98-4487 (1998).